ELSEVIER

Biophysical Chemistry 67 (1997) 159–165

Biophysical Chemistry

Biphasic transitions of a hairpin hexanucleotide triplex DNA

Imshik Lee *, Wenli Deng, Linjing Yang, Chen Wang, Chunli Bai

Institute of Chemistry, The Chinese Academy of Sciences, Beijing 100080, P.R. China

Received 10 December 1996; revised 13 March 1997; accepted 14 March 1997

Abstract

The conformational transitions (helix–coil transitions) of three hairpin triple helices, models 5′-(A-G)$_3$ + 5′-(T-C)$_3$-T$_4$-(^{br}C-T)$_3$ [CY], 5′-(A-G)$_3$ + 5′-(T-^{br}C)$_3$-T$_4$-(C-T)$_3$ [YC] and 5′-(A-G)$_3$ + 5′-(T-^{br}C)$_3$-T$_4$-(^{br}C-T)$_3$ [YY], are characterized in this work by UV spectroscopy. Melting of these triplexes is biphasic, and the profiles are used to obtain the thermodynamic parameters. The thermodynamic properties of the hairpin triplex are T_m = 19.45°C and ΔH_{vH} = 293.12 kJ mol^{-1} for CY, T_m = 22.85°C and ΔH_{vH} = 256.63 kJ mol^{-1} for YC and T_m = 28.47°C and ΔH_{vH} = 234.68 kJ mol^{-1} for YY at pH 4.4. Those of the duplex are T_m = 30.50°C and ΔH_{vH} = 427.09 kJ mol^{-1} for CY, T_m = 32.96°C and ΔH_{vH} = 374.47 kJ mol^{-1} for YC and T_m = 33.24°C and ΔH_{vH} = 329.67 kJ mol^{-1} for YY at pH 4.4. The distinct transitions of triplex to duplex and duplex to single strands are analyzed using the nearest-neighbor Ising model. Electrostatic effects on each conformation are also analyzed. © 1997 Elsevier Science B.V.

Keywords: Conformational transitions; Hairpin triplex DNA; UV spectroscopy; Electrostatic effects

1. Introduction

Since triplex DNA structures were observed in combinations of Watson–Crick base-paired double strands and the addition of a suitable third strand [1,2], vast attention has been focused on the biology and on novel approaches to therapeutics [3,4]. However, for successful pharmaceutical and clinical applications some aspects [5] need to be considered such as stability and molecular recognition. Several methods have investigated to improve the stability of triplex formation: modification of the backbone, such as substitution of methylphosphate or methylphosphorothioate, PNA (peptide nucleic acids) [6] or synthetic polymer [7]; modification of aromatic bases, such as substitution of protonated cytosine and/or 5-methylatecytosine [8]; and control of the environmental properties of DNA, such as changing the acidity of DNA solution, adding electrolytes or adding intercalators.

In the present work we have investigated the stability of triple-stranded DNA helices of appropriate sequence formed by the addition of a suitable third strand to a homopolypurine–homopolypyrimidine Watson–Crick type double helix [1,2]. Our objective was to evaluate the effect of substituting 5-bromocytosine(^{br}C) for cytosine on triplex stability in three different triplexes formed from the interaction of 5′-(A-G)$_3$ with 5′-(T-C)$_3$-T$_4$-(^{br}C-T)$_3$ [CY], 5′-(T-^{br}C)$_3$-T$_4$-(C-T)$_3$ [YC] and 5′-(T-^{br}C)$_3$-T$_4$-(^{br}C-

* Corresponding author.

PII S0301-4622(97)00038-0

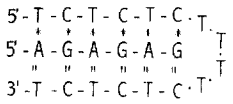

Fig. 1. Schematic diagram of a hairpin triple helical DNA. The Hoogsteen base pairs and Watson–Crick base pairs are marked by * and " respectively.

$T)_3$ [YY], with the aid of UV melting profiles. Fig. 1 shows an example of such a triplex. Thermodynamic parameters for triplex formation of CY, YC and YY were extracted from an analysis of the shape of the melting profiles [9,10].

2. Material and methods

2.1. Sample preparation

All oligodeoxynucelotides CY, YC and YY were synthesized and purified as previously described [11]. Hairpin triplexes were prepared by mixing equimolar amounts of the oligodeoxypurine $(A\text{-}G)_3$ with the corresponding oligodeoxypyrimidines, CY, YC and YY. Mixtures (2 μM oligomer) in 500 mM NaCl and 10 mM sodium phosphate buffers (pH 4.4) were first tested to 85°C and then slowly cooled to 4°C to ensure complete hairpin triplex formation. pH was measured using a Hanna pH meter with an HI8417 microcombination electrode.

2.2. UV measurements

UV absorbance was measured using a Hitachi V-3200 spectrophotometer and 1 cm pathlength quartz cells. The rate of temperature increase was 0.3–0.35°C min^{-1}.

For the pH stability studies, 1 ml solution containing 500 mM NaCl, 10 mM sodium phosphate and the triplex of interest was adjusted to different pH values using either HCl or NaOH. The pH stability data were collected at room temperature and plotted as a function of pH by measuring absorbence changes at 260 nm. Absorption spectra were corrected for any volume changes due to acid or base addition. pH was measured for all solutions before the absorption spectra were measured.

2.3. Melting profiles

Fig. 2 shows the melting profiles at 260 nm for the three hairpin triplexes. Each profile shows that melting is biphasic, the first presumably due to the dissociation of the third strand segment of the hairpin and the upper transition to the dissociation of the $(A\text{-}G)_3$ strand from its complement in the homopyrimidine strand. Such biphasic melting is characteristic of polynucleotide triplexes at lower ionic strength [12]. Changes in hypochromicity observed for the first transitions of CY, YC and YY are respectively 13.89%, 15.24% and 12.54% at pH 4.4, which seems reasonable given that the few T residues in the loop are not H bonded.

The experimental melting profile can be converted to a plot of α vs temperature, where α is the helix–coil transition fraction. In detail, we can normalize the UV transitions by taking the ratio at each temperature of the height between the experimental curve $A_{260}(T)$ and the lower baseline $A_D(T)$ and the height between the lower $[A_D(T)]$ and upper $[A_U(T)]$ baselines, i.e. $\alpha(T) = (A_{260}(T) - A_D(T))/(A_U(T) - A_D(T))$. Fig. 3 shows the normalized profiles of α vs temperature for the three different hairpin triplexes.

The van't Hoff enthalpy can be calculated from the UV melting profiles on the basis of the relation $\Delta H_{v\text{-}H} = 2(n+1)RT_m^2(\partial\alpha(T)/\partial T)_{T=T_m}$, where R is the universal gas constant and n is the number of strands that form the helical complex [10]. The melt-

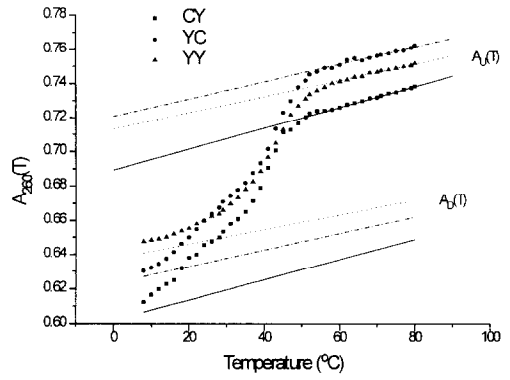

Fig. 2. Thermal denaturation profile $A_{260}(T)$ obtained from each 2.0 μM hairpin triplex DNA at pH 4.4. A_D indicates the lower baseline and A_U the upper baseline.

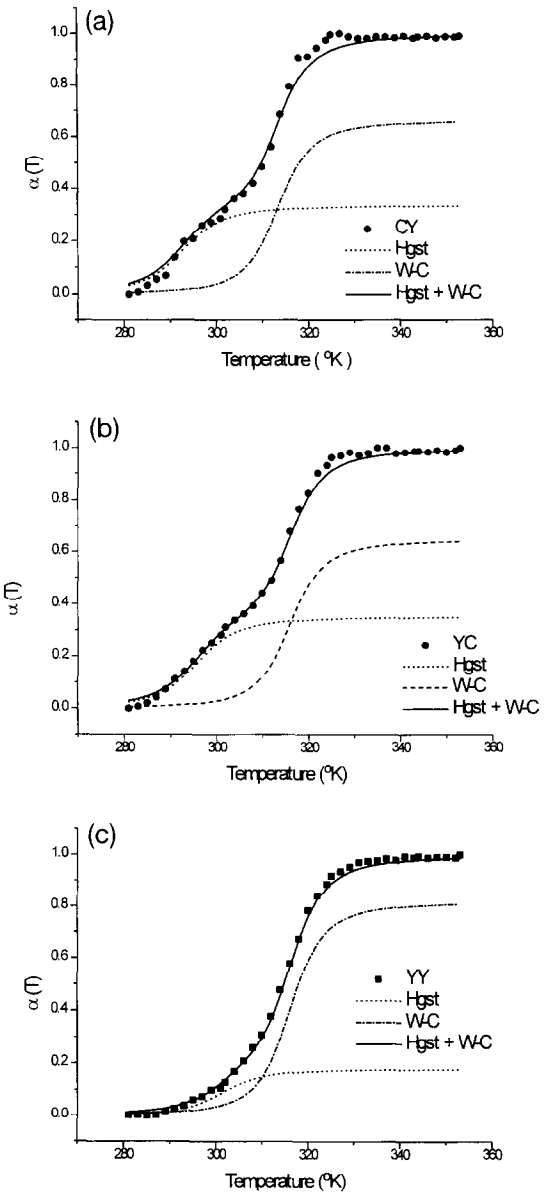

Fig. 3. Helix–coil transition α vs temperature T converted from Fig. 1. The profile of $d\alpha/dT$ vs temperature shows two peaks, indicating that two transitions occur in the thermal denaturation process. Watson–Crick and Hoogsteen base pairs are breaking at different levels. (a) CY, (b) YC and (c) YY. Empirical data are displayed as points and theoretical calculations as lines.

ing of CY, YC and YY occurs in biphasic transitions representing dissociation from triplex to duplex to single strands, similarly to triplex DNA. Table 1 shows the biphasic van't Hoff transition enthalpy values extracted from Figs. 2 and 3. T_m appears clearly different to that of the duplex (Watson–Crick) T_m point.

We have applied the theoretical nearest-neighbor Ising model [13] to the conformational transitions. To account for the fact that the Watson–Crick double-helical formation is a bimolecular reaction, the model considers the process from coil to Watson–Crick helix and coil (Watson–Crick transition):

$$CC \underset{s^{W-C}}{\leftrightarrow} H^{W-C}C$$

where s^{W-C} indicates the statistical weight $\exp(-\Delta G_{W-C}/RT) = \exp\{(\Delta H_{W-C}/RT_m)(1 - T_m/T)\}$ with $\Delta G_{W-C} = G^{coil}_{W-C} - G^{helix}_{W-C}$. For a chain of N residues, the partition function will be

$$Z(N) = \frac{\lambda_1^N(1-\lambda_2) + \lambda_1^N(\lambda_1 - 1)}{\lambda_1 - \lambda_2} \quad (1)$$

where

$$\lambda_{1,2} = \frac{1 + s^{W-C} \pm \sqrt{(1-s^{W-C})^2 + 4\sigma s^{W-C}}}{2}$$

with a nucleation parameter σ. The fraction of residues, $\alpha(T)$, in the coil conformation at a temperature T will be given by

$$\alpha(T) = \frac{\partial \ln Z(N)}{N \partial \ln s}$$

In this work, we attempt to compare the calculated fraction with the normalized UV profile of the temperature-induced transition. Therefore, we ignore the dependency on molecular weight.

$$\alpha(T) \approx \frac{\partial \ln Z(N)}{N \partial \ln s^{W-C}}$$

$$= \left[s^{W-C}\left(\sqrt{(s^{W-C}-1)^2 + 4\sigma s^{W-C}} + (s^{W-C}-1) + 2\sigma\right)\right] / \left[\left\{(1+s^{W-C}) + \sqrt{(s^{W-C}-1)^2 + 4\sigma s^{W-C}}\right\} \times \sqrt{(s^{W-C}-1)^2 + 4\sigma s^{W-C}}\right]^{-1} \quad (2)$$

The transition process from coil and Watson–Crick helix to triple helix (Watson–Crick and Hoog-

Table 1
Conformational transition parameters for each hairpin triple helix, obtained from UV absorption. Hgst = Hoogsteen base pairs; W–C = Watson–Crick base pairs

	CY		YC		YY	
	T_m(K)	ΔH_{vH}(kJ mol^{-1})	T_m	ΔH_{vH}	T_m	ΔH_{vH}
Hgst	292.9 ± 1.8	293.12	295.8 ± 2.1	256.63	301.5 ± 2.3	234.7
W–C	313.5 ± 1.4	423.09	316.0 ± 1.6	374.47	316.2 ± 2.0	329.7

steen helix: Hoogsteen transition) will be described in the same manner as the Watson–Crick transition:

$$H^{W-C}C \underset{S^{Hgst}}{\leftrightarrow} H^{W-C}H^{Hgst}$$

These two processes are superimposed in the UV melting profile. The curves in Fig. 3 are based on theoretical calculations (lines). It can be seen that the theoretical calculations are consistent with the experimental data (points). In this theoretical calculation the electrolyte environment was not included. A counterion effect on the conformational transition is considered in the following section. The change of the Hoogsteen transition is discernible with the place of ^{br}C. The transition order of the Hoogsteen is CY < YY, which is the same as the order of the T_m values for the transition.

Table 2 summarizes the amplitude of each transition and a nucleation parameter (or cooperative parameter) σ obtained for CY, YC and YY. The σ values of the triplex transitions are slightly higher than those of the duplex transitions. If we assume that the amplitudes of the non-modified hairpin triplex DNA (CC) are A^{Hgst} for the Hoogsteen transition and A^{W-C} for the Watson–Crick transition, $A_{CC}^{Hgst} + A_{CC}^{W-C} = 1$. By modifying the C base to ^{br}C, the additional amplitude changes of the Hoogsteen and Watson–Crick transitions define a^{Hgst} and A^{W-C} respectively. For CY, the amplitudes will be

$$A_{CY}^{Hgst} = A_{CC}^{Hgst}/\left(A_{CC}^{Hgst} + A_{CC}^{W-C} + a^{W-C}\right)$$
$$= A_{CC}^{Hgst}/(1 + a^{W-C})$$
$$A_{CY}^{W-C} = \left(A_{CC}^{W-C} + a^{W-C}\right)/\left(A_{CC}^{Hgst} + A_{CC}^{W-C} + a^{W-C}\right)$$
$$= \left(A_{CC}^{W-C} + a^{W-C}\right)/(1 + a^{W-C})$$

for YC,

$$A_{YC}^{Hgst} = \left(A_{CC}^{Hgst} + a^{Hgst}\right)/(1 + a^{Hgst})$$
$$A_{YC}^{W-C} = A_{CC}^{W-Ct}/(1 + a^{Hgst})$$

and for YY,

$$A_{YY}^{Hgst} = \left(A_{CC}^{Hgst} + a^{Hgst}\right)/(1 + a^{Hgst} + a^{W-C})$$
$$A_{YY}^{W-C} = \left(A_{CC}^{W-C} + a^{W-C}\right)/(1 + a^{Hgst} + a^{W-C})$$

The unknown parameters can be extracted from Table 2: $A_{CC}^{Hgst} = 0.554$, $A_{CC}^{W-C} = 0.446$, $a^{Hgst} = -0.312$ and $a^{W-C} = 0.650$. The ratio of A_{CC}^{Hgst} to A_{CC}^{W-C} is consistent with the results (0.48 and 0.52 for CC triplex at pH 7.0) reported by Lavelle and Fresco [14]. ^{br}C plays a role in enforcing UV absorbancy in the duplex whereas it prohibits it in the triplex. These results show that the increment in stability depends upon both the location in the sequence and the number of ^{br}C. Biphasic melting is well fitted by theoretical calculations.

Table 2
Normalized transition parameters for the Hoogsteen and Watson–Crick base pairs, obtained for CY, YC and YY. The values of σ are obtained from $\sigma = \left\{\Delta H/\left[4RT_m^2(\partial\alpha(T)/\partial T)_{T=T_m}\right]\right\}^2$

		Amplitude	σ
CY	Hgst	0.336	3.6×10^{-6}
	W–C	0.664	3.9×10^{-6}
YC	Hgst	0.352	2.7×10^{-6}
	W–C	0.648	2.9×10^{-6}
YY	Hgst	0.181	2.1×10^{-6}
	W–C	0.819	2.3×10^{-6}

3. Electrostatic effects

The conformational transition from coil to helix is the result of two opposing tendencies: (1) from states of high energy to states of low energy, and (2) from states of low entropy to states of high entropy. The molar free energy G of the system reflects both tendencies, and the stable state is that with the lowest free energy. Therefore, when $\Delta G > 0$ the helix is

stable, whereas when $\Delta G = 0$ the two states are in equilibrium and the temperature is the transition (melting) temperature, or T_m value.

The free energy change ΔG of the system of a hairpin triplex DNA in electrolyte solution will be considered as the result of two contributions. One (ΔG_e) is due to the electrostatic interaction between the phosphate negative charges; the other (ΔG_0) is due to non-electrostatic interaction. The stabilizing effect of monovalent counterions is due to two actions: (1) screening of fixed charges by counterion clouds, and (2) specific binding of counterions to fixed charge sites. We have observed that as the counterion concentration is increased by increasing monovalent counterion concentration, ΔG_e decreases with increasing salt concentration. For $\Delta G_e = 0$, the transition temperature (T_m) may be determined by

$$\Delta G_0 = 0 = \Delta H_0 - T_{m0}\Delta S_0$$

or

$$T_{m0} = \Delta H_0/\Delta S_0$$

where T_{m0} is the transition temperature at $\Delta G = 0$. At $\Delta G = 0$, we can also imply

$$\Delta G_0 = \Delta H_0 - T_m\Delta S_0 = -\Delta G_e$$

Thus

$$T_m = (\Delta H_0 + \Delta G_e)/\Delta S_0 = T_{m0} + \Delta G_e/\Delta S_0 \qquad (3)$$

G_e is always negative for DNA, because of the repulsion between the fixed phosphate charges. Therefore, as the screening effect increases, the transition temperature T_m increases. Conversely, as the counterion concentration decreases, the transition temperature shifts to favor the formation of species of lower effective charge densities.

Approximately, the mole electrostatic free energy can be derived by integration of the screened-Coulomb potential energy function over all charge pairs in the structure [15]. ΔG_e is the work done by removing a phosphate of charge e on one strand against the electrostatic potential, ψ, induced by the other strand. Thus,

$$\Delta G_e = -e\psi$$

where e is the charge. Hill [16] illustrated ΔG_e by using the linearized Poisson–Boltzmann equation in cylindrical coordinates to obtain an expression of the form

$$G_e\frac{e^2}{DL}\left\{\frac{B_0(\kappa a)}{\kappa a B_1(\kappa a)} + \ln\left(\frac{a}{R}\right)\right\}$$

where $(\kappa^2 = 8\kappa e^2 NM)/(1000DkT)$, in which the screening parameter κ is proportional to $M^{1/2}$, N is the Avogadro number, D the dielectric constant, k the Boltzmann constant, and M the monovalent counterion concentration in mol l^{-1}. a, R and L are respectively the ionic exclusion radius, the radius of a cylinder and the length of a cylinder. $B_0(x)$ and $B_1(x)$ are modified Bessel functions. The mole electrostatic free energy will be expressed in terms of summation of the screened-Coulomb potential energy over all charge pairs and the resulting modified Bessel function in the low salt concentration ($\kappa a < 1$). For a random coil,

$$G_e^{coil} = \frac{Ne^2 z_p^2}{b_c D_c}(\ln \kappa b_c + \gamma)$$

and, for an n-strand helix,

$$G_e^{helix} = -\frac{Nne^2 z_p^2}{lD_h} \times \left(\ln\frac{\kappa l}{n} + \sum_{m=1}^{m=\frac{2\pi}{\beta}-1}\left(\kappa a \sin\frac{m\beta}{2}\right) + \frac{2\pi}{\beta}\gamma\right) \qquad (4)$$

where z_p is the monomeric phosphate charge, which is 1 for DNA, b_c and b_h ($= \beta l/2\pi$, with helical repeat length l and base rotaion fracture β) are respectively the distance between adjacent charges projected on the long axis of the cylinder for a coil and for a helix, and $\gamma = 0.5772$ is Euler's constant. By differentiating Eq. (4) with respect to log M with the assumption that $D_c \approx D_h$ ($= D$), we summarize as

$$dT_m/d\log M = \frac{2.3Ne^2 z_p^2}{2D\Delta S_0}\left(\frac{n}{b_h} - \frac{1}{b_c}\right) \qquad (5)$$

Fig. 4a shows the log M dependence for the duplex in triplex solution, confirming the decreasing

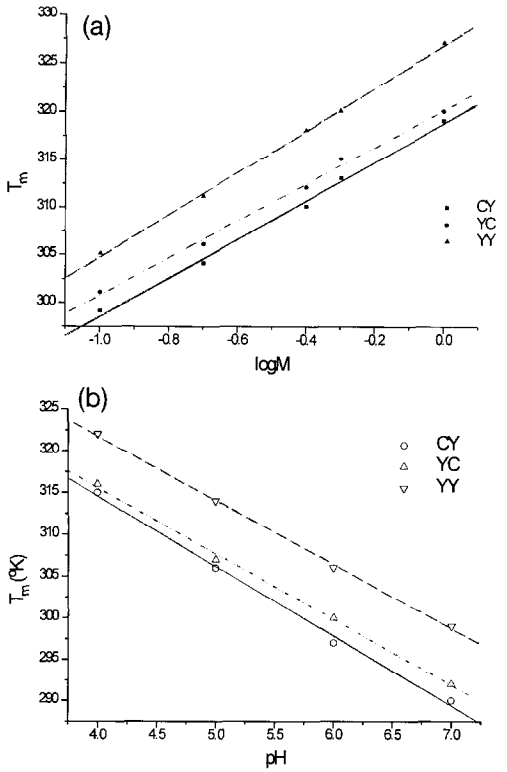

Fig. 4. (a) Variation of T_m with the logarithm of the molar NaCl concentration; for CY, T_{mCY} (K) = 20.26 log[M] + 318.85; for YC, T_{mYC} = 19.44 log[M] + 320.26; and for YY, T_{mYY} = 22.10 log[M] + 326.93. (b) Profile of T_ms of CY, YC and YY hairpin triplex DNA vs pH.

ionic strength of the solution. T_m for each conformation was determined to be a linear function of $dT_m/d\log M$; for the CY structure $dT_m/d\log M$ = 20.26, for YC 19.44 and for YY 22.09 at pH 4.4. This observation is similar to the results reported by Plum et al. [17]. The effect of Na^+ concentration seems to contribute to triplex stability by screening the negative charges of the phosphodiest backbones. The parameter D can be evaluated by Eq. (5) using the values $b_c = 6.8$ [18] and $b_h = 3.4$ (B-DNA). Dielectric constants of 8.38, 10.05 and 10.02 are obtained for CY, YC and YY, respectively. According to Table 1, the base pairs of triplex are more sensitive to the counterion concentration than are those of duplex. In the triplexes CY, YC and YY, $dT_m/d\log M$ values for the triplex base pairs are about 27.56 while those for the duplex base pairs are about 20.59. The salt dependence of triplex stability of poly(U:A.U) showed higher than that of duplex [19], which is similar to our observation. The order of the counterion concentration sensitivity ($dT_m/d\log M$) in the triplexes is YC(26.20) < CY(27.50) < YY(28.96), which is the same as the order of stability.

It is well known that the structure of the C:G.C triad is difficult to form at neutrality or above. Biologically relevant triplex formation should occur in vivo. In Watson–Crick, the G.C base pair is most strongly and accurately recognized, but the formation of the C:G.C triplet needs an additional protonation on N3 of C, enabling the formation of an additional hydrogen bond in the Hoogsteen base pair. Therefore, the formation of the C:G.C triplet is very sensitive to pH. The negative dependence of T_m on pH is displayed in Fig. 4b. The value of dT_m/dpH for CY, TC and YY is −8.4, −7.9 and −7.7 respectively. The pH sensitivity of the three different conformations is opposite to that of the conformational stability. Morever, the replacement of C with ^{br}C reduces the pH sensitivity. According to the relation [14] $\Delta(1/T_m)/\Delta(-pH) = -1.15R(\Delta n)/(Z\Delta H)$, the stoichiometric changes $\Delta n/Z$ in protonation on helix dissociation are obtained as 4.11, 3.35 and 2.76 for CY, YC and YY, respectively.

4. Summary

We have observed the biphasic temperature-induced transition of CY, YC and YY by UV melting profiles. The two transitions correspond to the triplex transition to duplex and the melting of duplex to single strands. Our theoretical analysis is consistent with experimental observations. Putting ^{br}C in place of C stabilizes triplexes. ^{br}C enforces UV absorbancy in duplex while inhibiting it in triplex, which shows that the increment in stability depends upon both the location in the sequence and the number of ^{br}C. The effect of Na^+ concentration seems to contribute to triplex stability by screening the negative charges of the phosphodiest backbones in general, but the replacement of C with ^{br}C reduces the pH sensitivity.

Acknowledgements

This work has been supported by the National Natural Science Foundation of P.R. China. I Lee is grateful for the support from the State Bureau of Foreign Experts.

References

[1] J.S. Lee, M.L. Woodsworth, L.J.P. Latimer, A.R. Morgan, Nucleic Acids Res. 12 (1984) 6603.
[2] G. Felsenfield, D.R. Davis, A. Rick, J. Am. Chem. Soc. 79 (1957) 2023.
[3] J.S. Cohen, TIBTECH 10 (1992) 87.
[4] E. Uhlmann, A. Peyman, Chem. Rev. 90 (1990) 543.
[5] C.A. Stein, Y.-C. Cheng, Science 261 (1993) 1004.
[6] J.C. Norton, M.A. Piatyszek, W.E. Wright, Nature Biochem. 14 (1996) 615.
[7] W.T. Smith Jr., Prog. Polym. Sci. 21 (1996) 209.
[8] Y.-K. Cheng, B.M. Pettitt, Prog. Biophys. Molec. Biol. 58 (1992) 225.
[9] W. Deng, I. Lee, Q. Li, L. Yang, C. Wang, C. Bai, E. Cao, L.-S Kan, to be published.
[10] L.S. Marky, K.J. Breslauer, Biopolymers 26 (1987) 1601.
[11] Y. Fang, C. Bai, Y. Wei, S.-B. Lin, L.-S. Kan, J. Biomol. Str. & Dyn. 13 (1995) 471.
[12] R.D. Blake, J. Massoulie, J.R. Fresco, J. Mol. Biol. 30 (1967) 291.
[13] D. Poland, H.A. Scheraga, Theory of Helix–Coil Transition in Biopolymers, Academic Press, New York, 1970.
[14] L. Lavelle, J.R. Fresco, Nucleic Acid Res. 23 (1995) 2692.
[15] M.T. Record Jr., Biopolymers 5 (1967) 975.
[16] T.L. Hill, Arch. Biochem. Biophys. 57 (1955) 229.
[17] E.G. Plum, Y.W. Park, S.F. Singleton, P.B. Dervan, K.J. Breslauer, Proc. Nat. Acad. Sci. USA 87 (1990) 9436.
[18] T. Ohnishi, Biophys. J. 3 (1963) 459.
[19] R.D. Blake, J. Massoulie, J.R. Fresco, J. Mol. Biol. 30 (1967) 291.